

All-Cellulose Composite Prepared by Selective Dissolving of Fiber Surface

Takashi Nishino* and Noriko Arimoto

Department of Chemical Science and Engineering, Faculty of Engineering, Kobe University, Rokko, Nada, Kobe 657-8501, Japan

Received March 27, 2007; Revised Manuscript Received June 30, 2007

An all-cellulose composite was prepared from conventional filter paper by converting a selective dissolved fiber surface into a matrix. The structure and mechanical, thermal, and optical properties of this composite were investigated using X-ray diffraction, a scanning electron microscope, an optical microscope, a tensile test, and dynamic viscoelastic analyses. After optimizing the immersion condition of the filter paper in a solvent, the fibers, with selectively dissolved surfaces, were unified by compression followed by drying. The tensile strength of the composite reached 211 MPa at 25 °C, isotropically. This value was comparable or even higher than those of conventional glass-fiber-mat-reinforced composites. The composites possessed a high storage modulus of more than 20 GPa at –150 °C, and a storage modulus of the GPa order was maintained up to around 250 °C. The good interface is considered to bring optical transparency to this composite. In addition, this composite is composed of sustainable resources and is biodegradable after service, which gives it advantages with regard to disposal, composting, and incineration.

Introduction

Composite materials have excellent mechanical and thermal properties; they are thus widely used in various applications ranging from aerospace to vehicles to sports equipment.¹ However, when disposing by incineration, these advantages bring about environmental issues. Consequently, there are growing demands for environmentally friendly composites.^{2–4}

Cellulose is the most abundant natural homopolymer, and it plays a significant role in the structural support of plant cell walls because of its high mechanical properties.⁵ Together with a relatively high elastic modulus of 138 GPa for the crystalline regions in the direction parallel to the chain axis⁶ and a high degree of polymerization, the linear orientation of native cellulose (cellulose I) molecules contribute to the mechanical high performance of the plant cell wall. In addition, inter/intrahydrogen bonds stabilize the molecule itself, and connect it tightly to neighboring ones. The maximum macroscopic Young's modulus of plant cellulose (up to 128 GPa)⁷ is higher than those of aluminum (70 GPa) and glass fiber (76 GPa). The excellent mechanical property of cellulose has brought about the current trend toward eco-composites focusing on the best use of cellulose fibers, e.g., poly-L-lactic acid reinforced with natural plant fiber (hemp,⁸ kenaf,⁹ flax,¹⁰ etc.).

In general, composites are composed of two chemically different materials. The interface between the incorporated fiber and the matrix often causes problems, such as poor compatibility, insufficient stress transfer, and high water uptake. If the fiber and the matrix are both made of the same material, benefits such as recyclability and good adhesion through the perfect interface can be expected. We were the first to report the development of a novel material, an all-cellulose composite, in which the incorporated fibers and the matrix were both made of cellulose.¹¹ It was prepared by impregnating a cellulose

solution into uniaxially aligned cellulose fibers. This all-cellulose composite had excellent mechanical properties and thermal performance. However, from the view point of processing, it is difficult to impregnate the cellulose solution into fibers, as even longer times do often not lead to better impregnation if the viscosity is too high.

In this study, we developed a convenient alternative process for the preparation of the all-cellulose composite. Cellulose fibers with selectively dissolved surfaces were unified by compression and then dried. This process was expected to lead to good fiber–fiber adhesion. Recently, Gindl et al. reported similar types of composites inspired by our previous work.^{12–14} Matsumura and Glasser prepared partially esterified pulp fibers. Using these fibers, they prepared a cellulosic composite in which the thermoplastic cellulose hexanoate phase formed a matrix reinforced with the core cellulose I by hot compaction.^{15,16} The composites had a modulus of 1.3 GPa and a tensile strength of 25 MPa. Their concept would be in line with the “selective melt” process developed for all-polyethylene composites by Ward and co-workers^{17,18} and those for all-polypropylene composites by Peijs and co-workers.^{19,20}

Looking back into the history of paper, this process resembles the ones for making parchment paper and vulcanized fiber, where cellulose fibers were treated with concentrated H₂SO₄ for the parchment paper²¹ and ZnCl₂ for the vulcanized fiber,²² followed by compression/rinsing/drying. They are now commonly used for cooking, lapping, and so on. Their tensile strength has been limited up to 120 MPa. However, we report here an all-cellulose composite with a much better performance, for example, a composite with a tensile strength of 211 MPa, which is greater than that of a conventional glass-fiber-mat-reinforced composite (GFRP).²³

A cell wall of a natural fiber is composed of a number of layers. Among these layers, the outer layers are known to be less ordered and poorly oriented. On the contrary, the microfibril orientation of the inner S2 layer plays an important role for the mechanical high performance of cellulosic fibers.²⁴ In this study,

* Corresponding author. Tel: +81-78-803-6164. Fax: +81-78-803-6198. E-mail: tnishino@kobe-u.ac.jp.

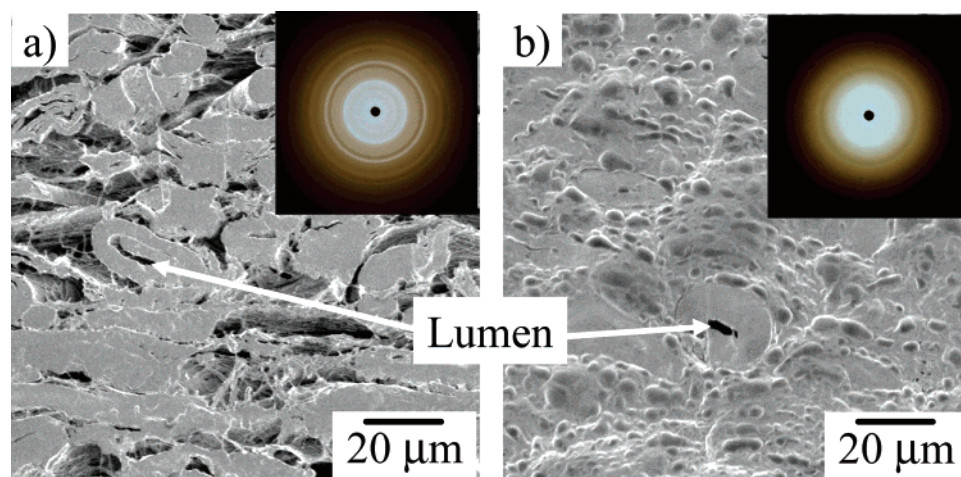


Figure 1. SEM micrographs of cross-sections of (a) the as-supplied filter paper and (b) the all-cellulose composite (12 h immersion). The X-ray diffraction photographs in the corners of the micrographs were taken from the direction perpendicular to the surface.

the surface less-ordered layer of the fibers was selectively dissolved and transferred into a matrix. This is suitable for providing high mechanical properties from the core fiber and good interfacial adhesion from the fiber surface. Thus, in order to find the optimum to fulfill these conditions, a systematic study on the sample preparation is required.

Here we report a systematic study on the structure and the mechanical, thermal, and optical properties of this type of all-cellulose composite.

Experimental Section

Sample Preparation. The cellulose source used in this study is a filter paper for quantitative chemical analysis (No. 5C, Toyo Roshi Kaisha, Ltd.; thickness: 0.22 mm; weight: 118 g/m²). The pretreatment was performed by immersing the filter paper in distilled water, acetone, and *N,N'*-dimethylacetamide (DMAc), each for 24 h at 25 °C, successively. Judging from an X-ray diffraction pattern of the filter paper, no structural change was observed after the pretreatment. Then, the pretreated filter paper was immersed in DMAc containing LiCl (8 wt %) solvent for the designated time at 30 °C.^{25,26} After that, the filter paper, with a selectively dissolved fiber surface, was compressed between poly(tetrafluoroethylene)-coated glass fiber sheets at 0.1 MPa for 1 h, followed by immersion in methanol to extract the DMAc and LiCl. During these processes, the fibers were unified and resolidified, and an all-cellulose composite was obtained. Finally, the all-cellulose composite was dried at 120 °C for 6 h, and further dried in a vacuum at 60 °C for 24 h. The effect of the immersion time in the solvent on the structure and properties of the final all-cellulose composite was investigated systematically. For example, the all-cellulose composite, made from a filter paper that had been immersed in the solvent for 12 h, is hereafter called the “all-cellulose composite (12 h immersion)”.

Measurements. X-ray diffraction photographs were taken by a flat camera having a length of 37.5 mm. The Cu K α radiation, generated with an RINT-2000 (Rigaku Co.) at 40 kV, 20 mA, was irradiated on the specimen perpendicular to the surface. The diffraction profile was detected using an X-ray goniometer with a symmetric reflection geometry. After subtracting the air scattering, the diffraction profile was curve resolved into noncrystalline scattering and crystalline reflections using Rigaku multi-peaks separation software. The apparent crystallinity, X_c , was evaluated from their area ratio. In this study, the fully dissolved/resolidified cellulose profile was regarded as the noncrystalline part.

The cross-section and the fracture surface of the composite were observed using a scanning electron microscope (SEM) (JSM-5610LVS (JEOL)), at an accelerating voltage of 20 kV. The cross-section was prepared by cutting the sample with a glass knife in the direction normal

to the sample surface. The fractured surface was observed after the tensile test. Pt/Pd was deposited on the surface prior to the observation.

The stress–strain curves of the filter paper and the all-cellulose composite were measured using a tensile tester (Autograph AGS-1kND, Shimadzu) at 25 °C for rectangular-shaped specimens with a thickness of several hundred micrometers. The initial length of the specimen was 10 mm, and the extension rate was 2 mm/min. A cross-sectional area was evaluated from the density, the weight, and the length of the sample. The average values and standard deviations of the Young's modulus and tensile strength σ_{max} were evaluated for five tested specimens. The dynamic storage modulus E' was measured by a dynamic mechanical analyzer (DVA-220S, ITK, Ltd.) from –150 to 300 °C. The measurements were performed in a nitrogen atmosphere to avoid thermal oxidation. A heating rate of 6 °C/min, an original length of 10 mm, and a frequency of 10 Hz were employed. A tensile deformation of 0.25% was applied to the specimen.

Prior to all the measurements, the specimen was conditioned at 120 °C for 20 min.

Results and Discussion

Figure 1 shows SEM micrographs of the cross-section of (a) the as-supplied filter paper and (b) the all-cellulose composite (12 h immersion). The X-ray diffraction photographs in the corners of the micrographs were taken from the direction perpendicular to the surface. A clear-cut cross-section of each fiber was observed for the filter paper, while they were hardly observed in the all-cellulose composite. This indicates that the fibers were completely unified in the composite by selective dissolving of the fiber surface and compression followed by resolidification, and the all-cellulose composite could be produced. The lumen, the hollow microtube inside the native plant fiber, remained at the center of the fiber in the composite, as shown by the arrows in the figures, which reveals that only the surface of the fiber had selectively dissolved. The X-ray diffraction photograph of the filter paper clearly showed Debye–Scherrer rings assigned as cellulose I modification. However, the diffraction pattern of the composite became diffuse, which suggests a decrease in the crystallinity by the selective dissolving/resolidification process.

Figure 2 shows the X-ray diffraction profiles of the filter paper and the all-cellulose composites at different immersion times up to 12 h. Clearly, the filter paper is composed of typical natural cellulose with a crystal modification of cellulose I, which shows

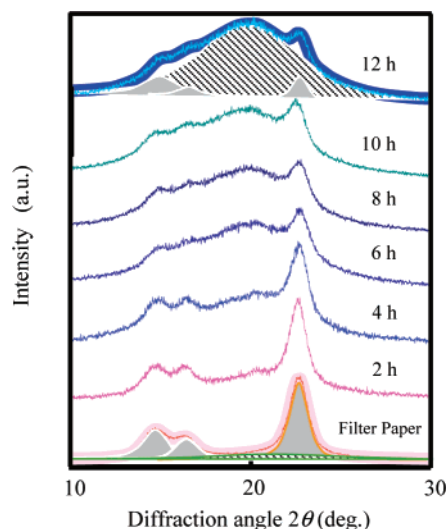


Figure 2. X-ray diffraction profiles of the filter paper and the all-cellulose composites at different immersion times up to 12 h. The gray area shows the crystalline 110, 1-10, and 200 reflections of cellulose I, and the hatched area corresponds to the noncrystalline scattering.

Table 1. The Apparent Crystallinity, X_c , Residual Fiber and Matrix Volume Percentages, and Fiber Diameter Change of the Filter Paper and the All-Cellulose Composites with Immersion Time

	filter	6 h	12 h
X_c (%)	86	19	14
residual fiber (vol %)	100	23	16
matrix (vol %)	0	77	84
diameter ratio d'/d^a	1	0.47	0.40

Cross section
image of fiber*

^a Assuming circular cross-section of cellulose fiber.

high crystallinity.²⁷ For the all-cellulose composites, as the immersion time in the solvent increased, the noncrystalline scattering apparently increased. This indicates that the dissolution of the cellulose fibers progressed gradually with the immersion time, and the resolidified part turned into noncrystalline regions in the composite. However, the main peaks at $2\theta = 22^\circ$ remained in all of the all-cellulose composite profiles. This indicates that the crystal modification of cellulose I was sustained in the composite, reflecting the existence of the residual fibers. In addition, the constant peak positions of the crystalline reflections indicate that the molecular distances remain unchanged in the crystalline regions. As previously mentioned, the filter paper had a high crystallinity, whereas the all-cellulose composites with longer immersion times possessed lower crystallinity. Thus, the percentage of residual fibers and the rate of change of the fiber diameters could be estimated from the change in crystallinity, assuming that all the fibers were hypothetically cylindrical in shape with the same diameters. The results of the curve fitting were superimposed on the figure for the as-supplied filter paper and the all-cellulose composite (12 h immersion), where the crystalline 110, 1-10, and 200 reflections were shown with the gray area, and the noncrystalline scattering was expressed with the hatched area. The fitted results coincided very well with the observed profile.

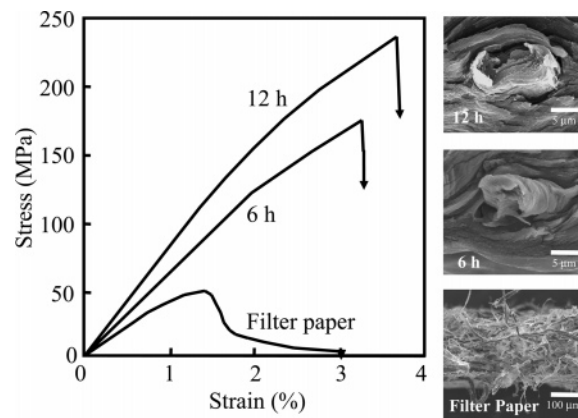


Figure 3. Stress–strain curves of the all-cellulose composites and the filter paper, together with the SEM micrographs of the fracture surface. The tensile tests were performed under dry conditions.

Table 1 shows the apparent crystallinity, X_c , residual fiber and matrix volume percentages, and the fiber diameter change of the filter paper and the all-cellulose composites with the immersion time. For simplification purposes, the diameter change and the schematic image of the fiber cross-section were evaluated using the following equation:

$$(d'/d) = (X'_c/X_c)^{0.5}$$

where, d and d' are the fiber diameters and X_c and X'_c are the apparent crystallinities before and after immersing the fiber in the solvent, respectively. The X_c value greatly decreased with the immersion of the filter paper in the solvent. For the all-cellulose composite (12 h immersion), 84% of the fiber was resolidified to form the matrix, and then 16% of the fiber remained.

Figure 3 shows the stress–strain curves of the all-cellulose composites and the filter paper, together with the SEM micrographs of the fracture surface. The Young's modulus, tensile strength, and elongation at the break were higher for the all-cellulose composites compared to those of the filter paper. The curve revealed that successive fractures occurred for the filter paper, which is caused by the disentanglement of the fibers as observed in the SEM micrograph. On the other hand, the all-cellulose composites showed brittle fractures, which implied an effective adhesion between the fibers. For the all-cellulose composite (6 h immersion), a fiber pull out from the matrix was observed, as shown in the SEM micrograph. This suggests that the fiber/matrix interface did not completely diminish but still existed in the composite. On the contrary, for the all-cellulose composite (12 h immersion), the fiber surface is efficiently dissolved, and the interdiffusion of the cellulose molecules across the interface was expected to be stimulated. This results in the simultaneous break-up of both the inner remaining fibers and the matrix, as shown in the SEM micrograph.

Figure 4 shows the Young's modulus, tensile strength, and crystallinity of the all-cellulose composites with different immersion times. For the all-cellulose composites (2 and 4 h immersion), the Young's modulus and tensile strength are lower than or similar to those of the filter paper. This is due to the decrease in crystallinity and insufficient dissolving to unify the fibers. When the immersion time became longer, the Young's

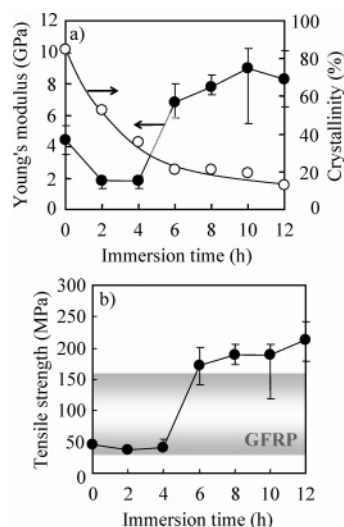


Figure 4. Relationship between the Young's modulus, tensile strength, crystallinity, and the immersion time for the all-cellulose composites.

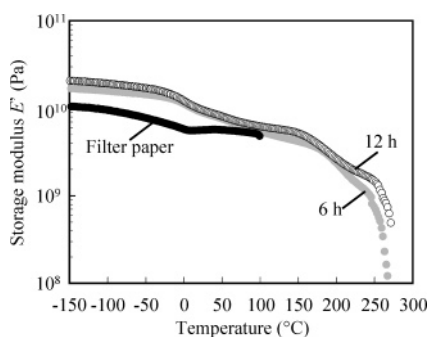


Figure 5. Temperature dependence of the dynamic storage modulus E' of the all-cellulose composites, together with that of the as-supplied filter paper.

modulus and the tensile strength increased. However, the amount of fiber that dissolved seemed to be higher for immersion times over 12 h, which made it difficult to keep the shape and process a uniform composite. After complete dissolving, a cellophane-cast film could be prepared, which showed a tensile strength of 50 MPa. With an immersion time of 12 h in the solvent, the all-cellulose composite showed especially high mechanical properties, for instance, a Young's modulus of 8.2 GPa and a tensile strength of 211 MPa. This tensile strength is higher than those reported by Gindl et al.^{12–14} and Glasser et al.,^{15,16} and is even higher than that of conventional GFRPs,²³ although the all-cellulose composite possesses much lower crystallinity than the original filter paper. These excellent properties are thought

to be due to the good fiber–fiber adhesion through an almost perfect interface.

Figure 5 shows the temperature dependence of the dynamic storage modulus E' of the all-cellulose composites (6 and 12 h immersion), together with that of as-supplied filter paper. The E' value of the all-cellulose composites possessed more than 20 GPa at $-150\text{ }^{\circ}\text{C}$ isotropically, which is higher than that of the filter paper and other conventional polymers, even without chain orientation. Furthermore, although the E' value of the all-cellulose composite decreased with an increase in the temperature, the drop was limited, and the high storage modulus of the GPa order was maintained up to around $250\text{ }^{\circ}\text{C}$. This thermal/mechanical performance is very high compared with that of other polymer-based composites. The elastic modulus of the crystalline regions of cellulose I is temperature independent,³ which contributes to the excellent thermal and mechanical properties of the all-cellulose composites.

Figure 6 shows optical photographs of the filter paper (a) and the all-cellulose composites (immersion times: (b) 6 h and (c) 12 h). The filter paper is white and opaque, while the all-cellulose composite with a longer immersion time in the solvent became transparent. Recently, Yano et al. reported optically transparent composites by combining bacterial cellulose with polymeric matrices. This transparency was attained because of the nanodimensional effect of the fibers.²⁸ On the other hand, the diameter of the fibers in this study is on the order of several tens of micrometers. Thus, the good interface, and the additional effect of the closure of the internal cell wall porosity by compression are thought to bring optical transparency to this composite.

The all-cellulose composite possesses a good interface between the remaining fibers and the surrounding matrix from the selectively dissolved/resolidified fiber, resulting in an excellent bonding, a high mechanical performance, and an optical transparency.

Conclusions

An isotropic all-cellulose composite was manufactured from conventional filter paper. This composite possessed a good interface between the remaining fibers and the surrounding matrix from the selectively dissolved/resolidified fiber surface, which results in the excellent bonding, high mechanical and thermal performance, and optical transparency of the composites. This prevents the typical interfacial issues for composites. The all-cellulose composite is totally composed of sustainable cellulosic resources, so it is biodegradable after service, which gives it advantages with regard to disposal, composting, and incineration.

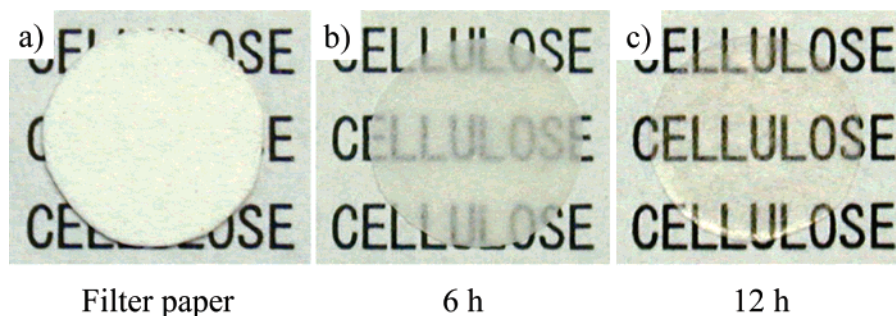


Figure 6. Optical photographs of filter paper (a) and all-cellulose composites (immersion times: (b) 6 h and (c) 12 h).

Acknowledgment. The authors would like to acknowledge the financial support by a Grant-in-Aid for Scientific Research from the Ministry of Education, Culture, Science, Sports and Technology, Japan (No.17310047).

References and Notes

- (1) Hull, D.; Clyne, T. W. *An Introduction to Composite Materials*, 2nd ed.; Cambridge University Press: Cambridge, U.K., 1996.
- (2) Bledzki, A. K.; Gassan, J. *Prog. Polym. Sci.* **1999**, *24*, 221.
- (3) Nishino, T. In *Green Composites*; Baillie, A. K., Ed.; Woodhead Publishing: Cambridge, U.K., 2004; p 49.
- (4) Bismarck, A.; Mishra, S.; Lampke, T. In *Natural Fibers, Biopolymers, and Biocomposites*; Mohanty, A. K., Misra, M., Drzal, L. T., Eds.; Taylor & Francis: Boca Raton, FL, 2005; p 37.
- (5) Bos, H. L.; Van Den Oever, M. J. A.; Peters, O. C. J. *J. Mater. Sci.* **2002**, *37*, 1683.
- (6) Nishino, T.; Takano, K.; Nakamae, K. *J. Polym. Sci., Part B.: Polym. Phys.* **1995**, *33*, 1647.
- (7) Page, D. T.; El-Hosseiny, F.; Winker, K. *Nature* **1971**, *229*, 252.
- (8) Panthapulakkal, S.; Sain, M. *J. Appl. Polym. Sci.* **2007**, *103*, 2432.
- (9) Nishino, T.; Hirao, K.; Kotera, M. *Composites, Part A* **2006**, *37*, 2269.
- (10) Singleton, A. C. N.; Baillie, C. A.; Beaumont, P. W. R.; Peijs, T. *Composites, Part B* **2006**, *34*, 519.
- (11) Nishino, T.; Matsuda, I.; Hirao, K. *Macromolecules*, **2004**, *37*, 7683.
- (12) Gindl, W.; Keckes, J. *Polymer* **2005**, *46*, 10221.
- (13) Gindl, W.; Martinschitz, K. J.; Boesecke, P.; Keckes, J. *Compos. Sci. Technol.* **2006**, *66*, 2639.
- (14) Gindl, W.; Schoberl, T.; Keckes, J. *Appl. Phys.* **2006**, *A83*, 19.
- (15) Matsumura, H.; Gugiyama, J.; Glasser, W. G. *J. Appl. Polym. Sci.* **2000**, *78*, 2242.
- (16) Matsumura, H.; Glasser, W. G. *J. Appl. Polym. Sci.* **2000**, *78*, 2254.
- (17) Ward, I. M.; Hine, P. J. *Polym. Eng. Sci.* **1997**, *37*, 1809.
- (18) Ward, I. M.; Hine, P. J. *Polymer* **2004**, *45*, 1413.
- (19) Alcock, B.; Cabrera, N. O.; Barkoula, N.-M.; Loos, J.; Peijs, T. *Composites, Part A* **2006**, *37*, 716.
- (20) Alcock, B.; Cabrera, N. O.; Barkoula, N.-M.; Reynolds, C. T.; Govaert, L. E.; Peijs, T. *Compos. Sci. Technol.* **2007**, *67*, 2061.
- (21) Atsuki, K. In *Chemistry and Industries of Cellulose*; Maruzen: Tokyo, 1956; p 244 (in Japanese).
- (22) Brown, W. F. *Proc. Electr. Insul. Conf.* **1999**, 309.
- (23) Sims, G. D.; Broughton, W. R. In *Polymer Matrix Composites*; Talreja, R., Manson, J.-A. E., Eds.; Elsevier Science: Oxford, U.K., 2001; p 151.
- (24) Rong, M. Z.; Zhang, M. Q.; Liu, Y.; Yang, G. C.; Zeng, H. M. *Compos. Sci. Technol.* **2001**, *61*, 1437.
- (25) Turbak, A. F. *Tappi J.* **1984**, *67*, 94.
- (26) Ishii, D.; Tatsumi, D.; Matsumoto, T. *Biomacromolecules* **2003**, *4*, 1238.
- (27) Nishiyama, Y.; Langan, P.; Chanzy, H. *J. Am. Chem. Soc.* **2002**, *124*, 9074.
- (28) Nogi, M.; Handa, K.; Nakagaito, A. N.; Yano, H. *Appl. Phys. Lett.* **2005**, *87*, 243110.

BM0703416